3rd China-Japan Joint Workshop on Positron Science (JWPS2017)
JJAP Conf. Proc. **7**, 011104 (2018) https://doi.org/10.7567/JJAPCP.7.011104

Defect Related Room Temperature Ferromagnetism in N-implanted ZnO Film

Juping Xu[1,2,3], Qiang Li[2,3], Bingchuan Gu[1], Jiandang Liu[1], and Bangjiao Ye[1*]

[1]*State Key Laboratory of Particle Detection and Electronics, University of Science and Technology of China, Hefei, 230026, China*
[2]*Institute of High Energy Physics, Chinese Academy of Sciences (CAS), Beijing 100049, China*
[3]*Dongguan Neutron Science Center, Dongguan 523803, China*

E-mail: bjye@ustc.edu.cn

(Received August 30, 2017)

Ion implantation was used to introduce N-ions into a ZnO film, which was deposited on sapphire by pulsed-laser deposition. The implantation fluence of N-ions was about 5×10^{16} cm^{-2}. The annealing behavior of ferromagnetism and structures of the N-implanted ZnO sample were determined by a vibrating sample magnetometer and X-ray diffraction, respectively. Positron annihilation spectroscopy and Raman spectroscopy were also employed to investigate the defect conditions in the sample. We observed that room temperature ferromagnetism can be introduced by V_{Zn}-related defect-complexes instead of only by substitutional N-ions. The results were supported by ab initio calculations based on density functional theory. Also, the possibility of oxygen vacancies as the origin of the ferromagnetism was clearly ruled out.

1. Introduction

ZnO-based dilute magnetic semiconductors (DMSs) have attracted increasing attention in the past years as promising candidates for spintronics [1]. However, the intricate magnetic mechanisms always result in diverse behavior of magnetism in experimental studies [2–5]. For instance, many reports demonstrated that Zn vacancies (V_{Zn}) are responsible for ferromagnetism in ZnO, while others considered the ferromagnetism should be attributed to ubiquitous oxygen vacancies (V_O) in metal oxide [6, 7]. Moreover, defects may introduce itinerant carriers, which could play an important role in magnetic coupling in ZnO [8]. For transition-metal doped DMSs, the clusters should be carefully characterized with the best available method, which has been presented in a recent study [9]. Nonmetallic-doping usually can avoid clusters in samples, and the analysis of magnetic origin is relative easy. Recently, some calculations demonstrated that C and N can introduce a localized moment of about 2 μB and 1 μB in ZnO lattices, respectively [10–12]. However, the magnetic coupling of C or N ions in ZnO is very different from that in other materials like MgO. Akbar et al. observed C-ions tend to combine with O-ions and form defect-complexes with V_{Zn}, which can only stabilize the ferromagnetic coupling among V_{Zn} [13]. Also, the N-related complex was reported in N-doped ZnO [14]. To further research defect-induced ferromagnetism in ZnO, we employed ion implantation to introduce N-ions and irradiated vacancy-defects in ZnO film. The structure and magnetic properties of the sample were determined by positron annihilation spectroscopy and vibrating sample magnetometry.

2. Experiment

We deposited ZnO films on sapphire substrates by pulsed-laser deposition. The thickness of the film was about 260 nm. The deposition process and conditions are described in Ref. [3]. Samples was cut into a size of 6 mm × 4 mm and carefully cleaned with ultrasonic acetone. Before implantation the film shows diamagnetic behavior at room temperature. Irradiation with N-ions at a fluence of

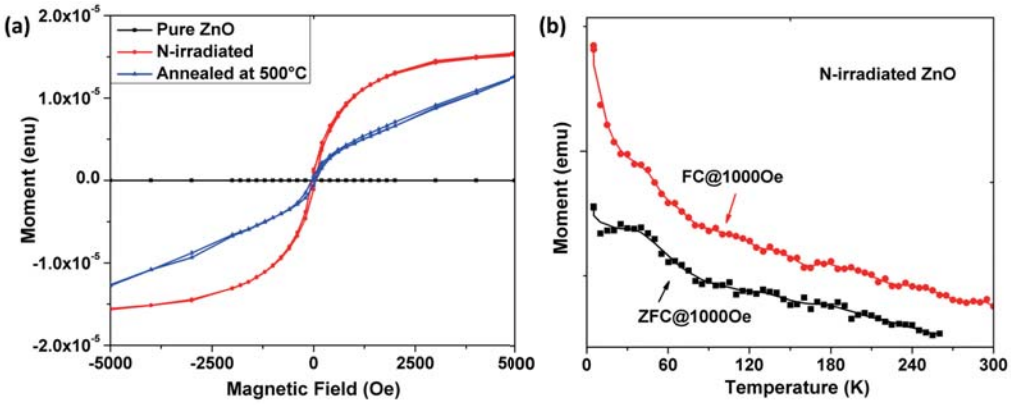

Fig. 1 (a) M-H curves at room temperature for N-irradiated ZnO film and the film annealed at 500 °C in nitrogen; (b) M-T curves measured in field-cooling and zero field-cooling (FC/ZFC) under 1000 Oe for N-irradiated ZnO.

5×10^{16} cm^{-2} was performed using the 100 keV Electro-magnetic Isotope Separator at the Shanghai Institute of Applied Physics (SIAP). Room-temperature magnetic properties were obtained using a Vibrating Sample Magnetometer (VSM) with an accuracy of 10^{-7} emu. The structure and defects of the irradiated sample were demonstrated by X-ray diffraction spectroscopy and slow positron annihilation measurements. Raman spectra were employed to analysis the structure vibration modes in sample. After implantation, the film was annealed at 500 °C in nitrogen to further reveal the relevance between magnetism and structure. Annealing at 500 °C may greatly change the vacancy density in N-implanted ZnO film without affect the vacancy-impurity complexes.

3. Results and discussion

Figure 1(a) and 1(b) show 300 K field-dependent magnetization (M-H) and temperature dependent magnetization (M-T) curves, respectively. The diamagnetic background of as-grown ZnO film in Fig. 1(a) is displayed as a horizontal line, which was subtracted from the other curves.

Room temperature ferromagnetism was clearly observed in N-irradiated ZnO film. The saturated magnetization is about 0.42 emu g^{-1}. An M-H curve which is approximately parallel to X-axis at fields larger than 5000 Oe indicates an absence of paramagnetic behavior in the sample. A coercive field (H_C) can be identified at lower magnetic field (-200 Oe $\sim$ H $\sim$ 200 Oe). H_C is attributed to ferromagnetic coupling in the sample. Before annealing, M-T curves in field-cooling and zero field-cooling (FC/ZFC) under 1000 Oe, were measured and are shown in Fig. 1(b). The FC/ZFC points display a slow decrease with increasing temperature from 5 K to 300 K. There is no coincidence or TC inflection, indicating that the Curie temperature of this film is larger than 300 K. FC/ZFC curves show slight platform at temperatures under 45 K, and the value of H_C/M_S is lower than normal soft magnetic materials. However, this is far different from the situation of superparamagnetism in Co-doped ZnO systems [15]. The H_C/M_S value measured at 10 K is no larger than that obtained at room temperature. We can exclude super paramagnetic or spin glass behavior in the sample. This is in good agreement with previous report on ZnO films deposited under N_2 gas ambience [16]. As shown in Fig. 1(a), the magnetization was reduced by around 70 % after the sample was annealed at 500 °C and the M-H curve show paramagnetic behavior at fields larger than 1000 Oe. This may be because ferromagnetism was interrupted and many localized moments turn to isolated states, which will reduce the value of ferromagnetism at room temperature.

We employed 18 kW rotating anode X-ray diffraction to characterize the structure and results are shown in Fig. 2. In addition to substrate diffraction, the sample shows only ZnO (002) and (004)

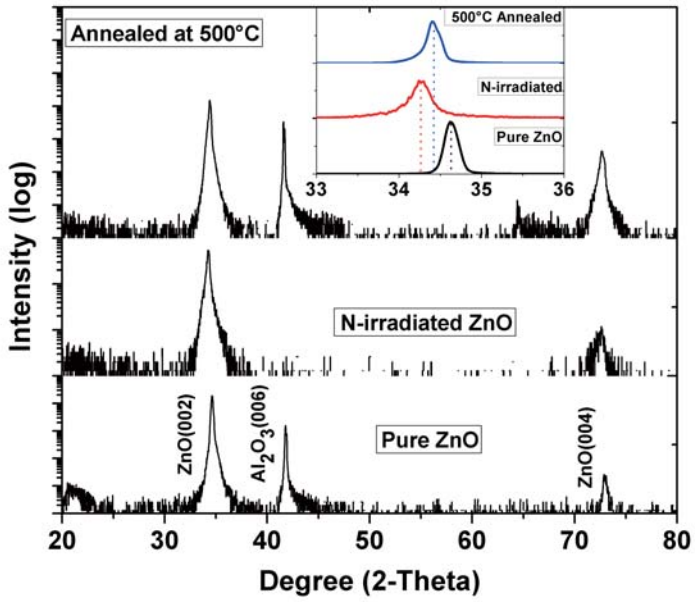

Fig. 2 XRD patterns of N-irradiated ZnO film and the film annealed at 500 °C. The inset is enlarged region of ZnO (002) peak of this film.

peaks corresponding to wurtzite hexagonal structure. No extra second-phase diffraction peaks were observed in the N-irradiated sample. The inset in Fig. 2 shows the (002) peak shifts to a lower angle by about 0.4° and the full width at half-maximum (FWHM) of this peak shows a slight broadening after N-irradiation, indicating a lattice disorder due to irradiation induced defects. After annealing, this peak shift back to a higher angle although not yet coincident with the as-grown ZnO film. This shift of the (002) peak may be indicative of lattice repair, while the annealing did not eliminate all the defects in the film at 500 °C.

Figure 3(a) displays room temperature Raman spectra in the range from 80 cm^{-1} to 900 cm^{-1}. A volume of the 514.5 nm line from an Ar^+ ion laser was used for excitation. Compared with pure ZnO films (which have been clearly described in Ref. [3]), a relatively larger intensity of the A_1^{LO} mode (580 cm^{-1}) was observed in the N-irradiated ZnO film and other peaks are relatively unchanged. Meanwhile, an additional mode located at 276 cm^{-1} and apophysis at 130 cm^{-1} was also observed after N-irradiation. The 276 cm^{-1} peak intensity was shown to increase with increasing dose of N-ions [17]. This peak is only observed in N-ion irradiated ZnO films, indicating that the mode is relevant to appearance of doped N-ions. The intensity increase of the 580 cm^{-1} peak is due to V_O-related complex defects induced in ZnO lattice by N-irradiation [15]. It rapidly decreased after 500 °C annealing, while the intensity of other modes showed a slight increase. This indicates that the sample lattice was repaired and the V_O-related vacancies virtually eliminated after annealing. An electron paramagnetic resonance (EPR) spectrum, which is an effective tool for detecting unpaired electrons, of ZnO is shown in the inset to Fig. 3(a). A perfect ZnO crystal is a diamagnetic material which typically shows no EPR response. The N-implanted ZnO film show an obvious EPR response with a Lande factor (g) of 1.9968, which is approaching the charged state of V_O. According to previous reports, we infer this EPR signal may originate from the charged V_O on the surface or grain boundaries of ZnO film with $S = 1/2$ due to one lost electron [18]. The EPR signal fades away after the sample was annealed at 500 °C, due to annealing-induced recombination of unstable V_O^{+1}. Recombination may be caused by reposition of deflecting O-ions or the surface adsorbed O_2 into crystals by

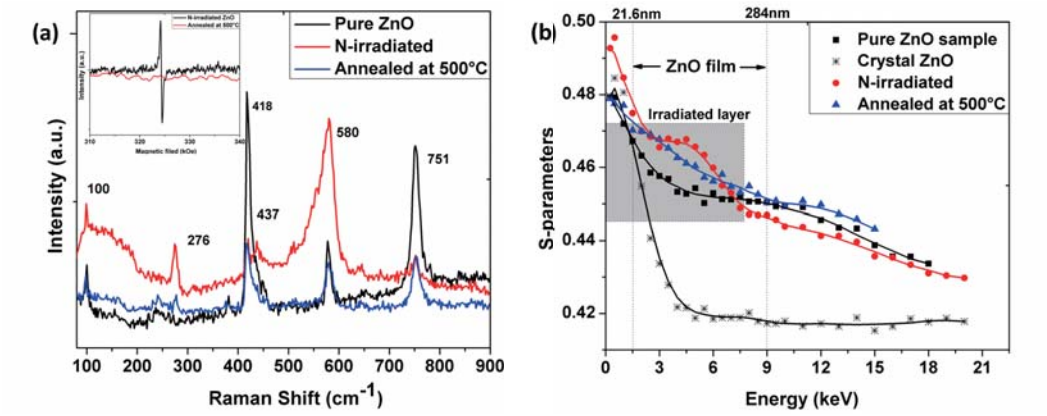

Fig. 3 (a) Room-temperature Raman spectra for N-irradiated ZnO film and the film annealed at 500 °C. The inset shows electron paramagnetic resonance (EPR) spectra. (b) S parameter as a function of positron implantation energy (S-E curves) for the N-irradiated and 500 °C annealed sample.

thermal annealing. Given the result of magnetic experiments, although the ferromagnetism appears after N-irradiation, the samples still show residual ferromagnetism and lots of isolated moments after annealing at 500 °C. The ferromagnetic behavior does not correspond to the changes of oxygen-related vacancies. The Raman apophysis located at 130 cm^{-1}, might arise from a disordered phase of ZnO, and was eliminated by sample re-crystallization after annealing [19]. Wang et al. calculated the density of states of local phonons in N-doped ZnO, and considered the 276 cm^{-1} mode is probably attributable to N-related defect-complexes [20]. This was confirmed by Chen et al. in a study of N-implanted ZnO crystals using positron techniques [14]. This peak was greatly reduced after 500 °C annealing, due to disintegration of the N-composited defects.

As a sensitive tool for detecting cation vacancies in materials, positron annihilation spectroscopy was employed to detect V_{Zn}-related defects in the sample. The measurements were carried out using a mono-energetic positron beam, with a positron energy from 0.25 keV to 20 keV. Positrons are easily trapped by vacancy defects and this results in a narrowing of the 511 keV annihilation peak compared to bulk annihilation. The S parameter was defined as the fraction of counts in the central region of this 511 keV peak [21]. Therefore, positrons annihilating in vacancies will result in an increase in the S parameter. As shown in Fig. 3(b), the S parameters of the as prepared ZnO film are greater than that of single crystal ZnO due to the grain interfaces in the deposited film. After irradiation, S parameters obviously increase. Based on VEPFIT analysis, the shaded region in Fig. 3(b) displays the irradiation layer, which corresponds to a positron energy from 1.55 keV to 7.5 keV [22]. The increase in S parameter in this layer should be attributed to Zn-related vacancies. Also, N-related vacancy-impurity complexes can lead to an increase in the S parameter. After annealing, the S parameter decreases but is still greater than that of as-deposited sample. This indicates that the sample still contains Zn-related vacancies after annealing, which can only be eliminated under higher temperature annealing, as demonstrated in a previous experiment [14].

The ZnO film shows room temperature ferromagnetism after N-implantation and a lot of vacancy-related defects were introduced into the sample. After 500 °C annealing, the ferromagnetism show a certain degree of decrease while the V_O almost disappeared. In contrast, V_{Zn} related defects remain after annealing. The result implies that remnant magnetization after annealing cannot be explained by effect of V_O. However, the annealing behavior of ferromagnetism is consistent with N-composited defects and V_{Zn}, which are considered relevant to the origin of magnetism. The ZnO film with grain interfaces shows diamagnetic behavior, while ferromagnetism was induced by implantation of N-

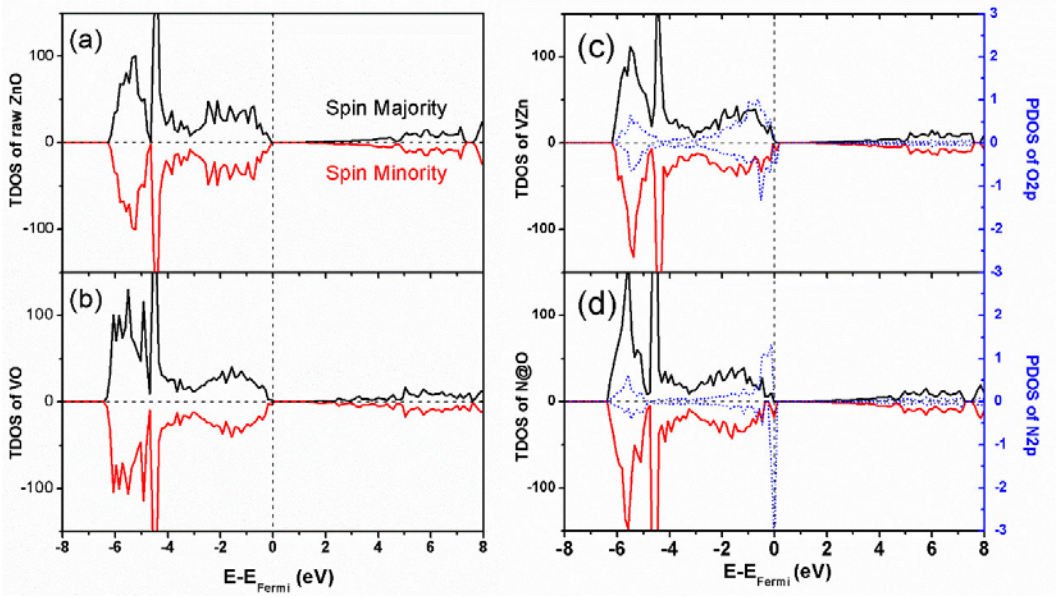

Fig. 4 The total density of state for the perfect ZnO crystal (a), with an V_O (b), a V_{Zn} (c) and a N-institution (d). The blue dashes in (c) and (d) display partial density of state for O2p state around V_{Zn} and N2p state for N-institution, respectively.

ions and a corresponding increase of V_{Zn}. It indicates that the N-impurities may play a role. To obtain further insight into the ferromagnetism in the implanted ZnO samples, a series of first-principle calculations based on density-functional theory were performed using the Vienna Ab-initio Simulation Package (VASP) [23, 24]. The magnetic properties in different structures of the ZnO supercell were calculated. The generalized gradient approximation with Perdew-Burke-Ernzerhof (PBE) functional was used to describe the exchange correlation energy and $4 \times 4 \times 4$ Monkhorst-Pack k-points of the Brillouin zone were used for structural optimization and static computation process [25, 26]. The cutoff energy was set to 400 keV and the relaxed Hellman-Feynman force on each ion was less than 0.01 eV Å^{-1}. The calculation was based on a 2×2 supercell which contains 32 O-atoms and 32 Zn-atoms. The cases of a N substitutional or a V_O/V_{Zn} at the center of the super-cell were taken into account and the results are shown in Fig. 4 and Table 1.

As shown in Fig. 4(a), the total and partial density of states (DOSs) for a perfect ZnO crystal has a symmetric spin density distribution, which indicates strict diamagnetic behavior in the ZnO material. In the structure with an O atom taken away, it is clear that the V_O with symmetric DOSs distribution does not introduce magnetism. As shown in table, the calculated magnetic moment is nearly zero. From the calculation, V_O^{+1} may induce a local moment in ZnO, it is then unstable within the ZnO crystal and tends to convert into neutral or (+2) charged states, which are non-magnetic. For the system to contain a neutral V_{Zn}, the spin-polarized states are generated near the top of the valence band and the whole supercell shows local magnetic moments with about 1.80 μB per V_{Zn}. The partial DOS (blue dashed line) in Fig. 4(c) display splitting impurity bands at the Fermi level. This is mainly caused by the spin-polarization of O2p electrons around V_{Zn}, which are the origin of localized moments in the system. As shown in Fig. 4(d), N substitutional at O also can introduce magnetic moment with 0.88 μB in the supercell, and the partial DOS show a contribution of N2p electrons. This indicates that the moment is localized and from implanted N-ions. However, its polarization energy is only about −23.5 meV which is smaller than the thermal disturbance energy at room temperature (~50 meV). The coupling polarization energy of two closed N ions is −39.9 meV, so it still cannot remain stable at room temperature. Thus, N impurities exhibit hardly any visible ferromagnetism at

Table I Magnetic moments (within the Wigner-Seitz radius) introduced by V_O, V_{Zn}, N_O, N_O-N_O and N_O-V_{Zn}-N_O different defected systems in ZnO supercell.

System	$Zn_{32}O_{31}$ (V_O)	$Zn_{31}O_{32}$ (V_{Zn})	$Zn_{32}O_{31}N$ (N_O)	$Zn_{32}O_{30}N_2$ (N_O-N_O)	$Zn_{31}O_{30}N_2$ (N_O-V_{Zn}-N_O)
Polarization energy [meV]	—	45.8	23.5	39.9	577.4
Magnetic moment [μB]	0.00	1.80	0.88	1.69	3.17

room temperature, although a local magnetic moment is contributed by N-ions in ZnO crystals. When V_{Zn} moderates the magnetic coupling between two N-ions, the a total magnetic moments show orientation consistency and the polarization energy is −577 meV. This value can make the sample resistant to thermal disturbances to exhibit room temperature ferromagnetism. The calculation results indicate that the room temperature ferromagnetism and remnant magnetization of the sample after annealing are related to V_{Zn}-related defect-complexes, N-ions may play a role in the origin of ferromagnetism. The results are in good agreement with our experiment discussed above.

4. Conclusion

In summary, room temperature ferromagnetism was observed in a N-irradiated ZnO film. After annealing the ferromagnetism shows a decrease in H_C and M_S, as well as a decrease in the concentration of V_{Zn} and N-composited defects detected by positron annihilation spectroscopy and Raman spectroscopy, respectively. In addition, oxygen vacancies (V_O) are almost eliminated after annealing, as demonstrated by Raman spectroscopy and electron paramagnetic resonance. The experimental and theoretical results confirm that the remaining ferromagnetism should be attributed to V_{Zn}-related defect-complexes, and exclude the effect of V_O. Also, the contribution of N-N magnetic coupling at room temperature was not supported by this work.

Acknowledgment

The authors are grateful for financial support from the National Natural Science Foundation of China (Grant Nos. 11175171 and 11475165).

References

[1] R. Kumar, F. Singh, B. Angadi, J.-W. Choi, W.-K. Choi, K. Jeong, J.-H. Song, M. W. Khan, J. P. Srivastava, A. Kumar, and R. P. Tandon, J. Appl. Phys. **100** 113708 (2006).
[2] D. Mukherjee, P. Mukherjee, H. Srikanth, and S. Witanachchi, J. Appl. Phys. **111**, 07C318 (2012).
[3] Q. Li, Y. Wang, J. Liu, W. Kong, and B. Ye, Appl. Surf. Sci. **289**, 42 (2014).
[4] G. Ciatto, A. Di Trolio, E. Fonda, P. Alippi, A. M. Testa, and A. A. Bonapasta, Phys. Rev. Lett. **107**, 127206 (2011).
[5] D. Li, D. K. Li, H. Z. Wu, F. Liang, W. Xie, C. W. Zou, L. X. Shao, J. Alloy. Compd. **591** (2014) 80-84.
[6] K. Rainey, J. Chess, J. Eixenberger, D. A. Tenne, C. B. Hanna, and A. Punnoose, J. Appl. Phys. **115**, 17D727 (2014).
[7] T.-L. Phan, Y. D. Zhang, D. S. Yang, N. X. Nghia, T. D. Thanh, and S. C. Yu, Appl. Phys. Lett. **102**, 072408 (2013).
[8] N. A. Spaldin, Phys. Rev. B **69**, 125201 (2004).
[9] M. Khalid, A. Setzer, M. Ziese, P. Esquinazi, D. Spemann, A. Pöppl, and E. Goering, Phys. Rev. B **81** (2010) 214414.

[10] H. Pan, J. B. Yi, L. Shen, R. Q. Wu, J. H. Yang, J. Y. Lin, Y. P. Feng, J. Ding, L. H. Van, and J. H. Yin, Phys. Rev. Lett. **99**, 127201 (2007).
[11] X. Xue, L. Liu, Z. Wang, and Y. Wu, J. Appl. Phys. **115**, 033902 (2014).
[12] H. Wu, A. Stroppa, S. Sakong, S. Picozzi, M. Scheffler, and P. Kratzer, Phys. Rev. Lett. **105**, 267203 (2010).
[13] S. Akbar, S. K. Hasanain, M. Abbas, S. Ozcan, B. Ali, and S. I. Shah, Solid State Commun. **151**, 17 (2011).
[14] Z. Q. Chen, T. Sekiguchi, X. L. Yuan, M. Maekawa, and A. Kawasuso, J. Phys.-Condes. Matter **16**, S293 (2004).
[15] Q. Li, Y. Wang, L. Fan, J. Liu, W. Kong, and B. Ye, Scr. Mater. **69**, 694 (2013).
[16] Q. Xu, H. Schmidt, S. Zhou, K. Potzger, M. Helm, H. Hochmuth, M. Lorenz, A. Setzer, P. Esquinazi, C. Meinecke, and M. Grundmann, Appl. Phys. Lett. **92**, 082508 (2008).
[17] Z. Hang, W. Z. Guang, P. L. Long, W. K. Fang, Y. C. Feng, S. T. Long, S. J. Rong, M. Y. Zhun, G. Jie, S. Y. Bin, and Z. Y. Bin, Nucl. Phys. Rev. **27**, 87 (2010).
[18] L. S. Vlasenko and G. D. Watkins, Phys. Rev. B **72**, 035203 (2005).
[19] J. Kennedy, B. Sundrakannan, R. S. Katiyar, A. Markwitz, Z. Li, and W. Gao, Curr. Appl. Phys. **8**, 291 (2008).
[20] J. B. Wang, H. M. Zhong, Z. F. Li, and W. Lu, Appl. Phys. Lett. **88**, 101913 (2006).
[21] J. Toivonen, T. Hakkarainen, M. Sopanen, H. Lipsanen, J. Oila, and K. Saarinen, Appl. Phys. Lett. **82**, 40 (2003).
[22] A. van Veen, H. Schut, J. de Vries, R. A. Hakvoort, and M. R. Ijpma, AIP Conf. Proc. **218**, 171 (1991).
[23] W. Koch and M. C. Holthausen,A Chemist's Guide to Density Functional Theory (Wiley, VCH, Weinheim, 2001).
[24] G. Kresse and J. Furthmüller, Phys. Rev. B **54**, 11169 (1996).
[25] J. P. Perdew, K. Burke, and M. Ernzerhof, Phys. Rev. Lett. **77**, 3865 (1996).
[26] H. J. Monkhorst and J. D. Pack, Phys. Rev. B **13**, 5188 (1976).